



6 Ma age of carving Westernmost Grand Canyon: Reconciling geologic data with combined AFT, (U–Th)/He, and $^4\text{He}/^3\text{He}$ thermochronologic data



Carmen Winn^{a,*}, Karl E. Karlstrom^{a,*}, David L. Shuster^{b,c}, Shari Kelley^d, Matthew Fox^{b,c,e}

^a Department of Earth and Planetary Sciences, University of New Mexico, Albuquerque, NM, USA

^b Department of Earth and Planetary Sciences, University of California, Berkeley, CA, USA

^c Berkeley Geochronology Center, 2455 Ridge Road, Berkeley, CA, USA

^d New Mexico Bureau of Geology and Mineral Resources, New Mexico Institute of Mining and Technology, Socorro, NM, USA

^e Department of Earth Sciences, University College London, Gower Street, London WC1E 6BT, United Kingdom

ARTICLE INFO

Article history:

Received 16 November 2016

Received in revised form 27 June 2017

Accepted 29 June 2017

Available online 26 July 2017

Editor: A. Yin

Keywords:

Grand Canyon

apatite

thermochronology

(U–Th)/He

fission track

$^4\text{He}/^3\text{He}$

ABSTRACT

Conflicting hypotheses about the timing of carving of the Grand Canyon involve either a 70 Ma (“old”) or <6 Ma (“young”) Grand Canyon. This paper evaluates the controversial westernmost segment of the Grand Canyon where the following lines of published evidence firmly favor a “young” Canyon. 1) North-derived Paleocene Hindu Fanglomerate was deposited across the present track of the westernmost Grand Canyon, which therefore was not present at ~55 Ma. 2) The 19 Ma Separation Point basalt is stranded between high relief side canyons feeding the main stem of the Colorado River and was emplaced before these tributaries and the main canyon were incised. 3) Geomorphic constraints indicate that relief generation in tributaries and on plateaus adjacent to the westernmost Grand Canyon took place after 17 Ma. 4) The late Miocene–Pliocene Muddy Creek Formation constraint shows that no river carrying far-traveled materials exited at the mouth of the Grand Canyon until after 6 Ma.

Interpretations of previously-published low-temperature thermochronologic data conflict with these lines of evidence, but are reconciled in this paper via the integration of three methods of analyses on the same sample: apatite (U–Th)/He ages (AHe), $^4\text{He}/^3\text{He}$ thermochronometry ($^4\text{He}/^3\text{He}$), and apatite fission-track ages and lengths (AFT). HeFTy software was used to generate time–temperature (t – T) paths that predict all new and published $^4\text{He}/^3\text{He}$, AHe, and AFT data to within assumed uncertainties. These t – T paths show cooling from ~100 °C to 40–60 °C in the Laramide (70–50 Ma), long-term residence at 40–60 °C in the mid-Tertiary (50–10 Ma), and cooling to near-surface temperatures after 10 Ma, and thus support young incision of the westernmost Grand Canyon.

A subset of AHe data, when interpreted alone (i.e. without $^4\text{He}/^3\text{He}$ or AFT data), are better predicted by t – T paths that cool to surface temperatures during the Laramide, consistent with an “old” Grand Canyon. However, the combined AFT, AHe, and $^4\text{He}/^3\text{He}$ analysis of a key sample from Separation Canyon can only be reconciled by a “young” Canyon. Additional new AFT (5 samples) and AHe data (3 samples) in several locations along the canyon corridor also support a “young” Canyon. This inconsistency, which mimics the overall controversy of the age of the Grand Canyon, is reconciled here by optimizing cooling paths so they are most consistent with multiple thermochronometers from the same rocks. To do this, we adjusted model parameters and uncertainties to account for uncertainty in the rate of radiation damage annealing in these apatites during sedimentary burial and the resulting variations in He retentivity. In westernmost Grand Canyon, peak burial conditions (temperature and duration) during the Laramide were likely insufficient to fully anneal radiation damage that accumulated during prolonged, near-surface residence since the Proterozoic. We conclude that application of multiple thermochronometers from common rocks reconciles conflicting thermochronologic interpretations and the data presented here are

* Corresponding authors.

E-mail addresses: cwinn264@unm.edu (C. Winn), kek1@unm.edu (K.E. Karlstrom).

best explained by a “young” westernmost Grand Canyon. Samples spread along the river corridor also suggest the possibility of variable mid-Tertiary thermal histories beneath north-retreating cliffs.

© 2017 Elsevier B.V. All rights reserved.

1. Introduction to the “age of Grand Canyon” controversy

The 140-year-long controversy about the age of the Grand Canyon was initially posed in terms of the hypothesis that the Colorado River was older than the tectonic uplifts it carves across (Powell, 1875; Dutton, 1882) and an alternate hypothesis that a younger river became erosionally superimposed on older, deeper monoclinal structures (Davis, 1901). It has long been recognized that Laramide-aged deposits from north-flowing rivers were present in the westernmost Grand Canyon (Young, 1966; Elston and Young, 1991) and some workers have related these deposits to an “old”, Laramide-aged (~70 Ma) Grand Canyon (e.g. Wernicke, 2011). As more research in the area was done, early proponents of a “young” (<6 Ma) Grand Canyon (e.g. Babenroth and Strahler, 1945; Blackwelder, 1934; Longwell, 1946; Lucchitta, 1966, 1972; McKee et al., 1967; Strahler, 1948) based their conclusions on the locally-derived Miocene–Pliocene Muddy Creek Fm., which stipulates that no far-traveled material reached the Grand Wash Trough through the mouth of the Grand Canyon between ~13 and 6 Ma.

Low-temperature apatite thermochronology methods began to be applied to Grand Canyon incision by Naeser et al. (1989) and Kelley et al. (2001). Subsequent studies have included apatite fission track (AFT), (U–Th)/He ages (AHe), and $^4\text{He}/^3\text{He}$ thermochronometry ($^4\text{He}/^3\text{He}$) such that the combined data should resolve continuous t – T paths from ~110 °C to surface temperatures of 10–25 °C. AFT relies on the temperature sensitivity of annealing the damage done by spontaneous fission of ^{238}U to the crystal structure. An AFT age is determined by the number of these ‘fission tracks’ relative to the parent isotope, while the lengths of the tracks (i.e., the degree of shortening from a ~17 μm initial length) provide information about residence time in the partial annealing zone (110–60 °C; Ketchum et al., 2007). AHe dating is sensitive to temperatures of 90–30 °C, where apatite crystals begin retaining radiogenic ^4He at different temperatures depending on initial U and Th parent concentrations (Shuster et al., 2006; Flowers et al., 2009). $^4\text{He}/^3\text{He}$ thermochronometry provides additional information about a given sample’s continuous cooling path and is especially sensitive to the lowest resolvable temperatures of the three methods (Shuster and Farley, 2005). The datasets, individually and combined, can be used to constrain multiple time–temperature (t – T) cooling paths that predict the data within acceptable statistical confidence. Cooling paths are then related to burial depths by assuming values for surface temperature and geothermal gradient, which in this area are commonly assumed to be 10–25 °C surface temperatures and a 25 °C/km geothermal gradient (Wernicke, 2011; Karlstrom et al., 2014).

Wernicke (2011) hypothesized that a NE-flowing 70–80 Ma California River and then a SW-flowing 55–30 Ma Arizona River both followed the modern Colorado River’s current path through the Grand Canyon and carved the canyon to within a few hundred meters of its modern depth by ~50 Ma. In this hypothesis, the Colorado River “was not an important factor in the excavation of Grand Canyon”. Flowers and Farley (2012) noted a major difference between eastern and western Grand Canyon cooling histories but supported an “old” westernmost Grand Canyon and stated: “The western Grand Canyon $^4\text{He}/^3\text{He}$ and AHe data demand a substantial cooling event at 70–80 Ma, and provide no evidence for the strong post-6 Ma cooling signal predicted by the young canyon model.” Flowers and Farley (2013) further supported the conclu-

sion of “... apatite $^4\text{He}/^3\text{He}$ and (U–Th)/He (AHe) evidence for carving of the western Grand Canyon to within a few hundred meters of modern depths by ~70 million years ago (Ma)”.

Other workers have proposed a more complex landscape evolution for individual canyon segments (Fig. 1A, inset map). Laramide rivers flowed generally north across the Grand Canyon–Colorado Plateau region (McKee et al., 1967; Young, 2001), perhaps following the Hurricane fault system (Fig. 1; Karlstrom et al., 2014). Thermal histories generated by AHe and AFT data from Lee et al. (2013) and Karlstrom et al. (2014) indicated different cooling histories for rim and river-level rocks in the Eastern Grand Canyon before 25 Ma but similar temperatures after 15 Ma, indicating that no canyon existed in this segment until the incision of an East Kaibab paleocanyon at 25–15 Ma. Thermochronologic data from these studies and others (Warneke, 2015) also indicate that Marble Canyon was not incised until the past 5–6 Ma.

Karlstrom et al. (2014) proposed a “paleocanyon solution” whereby an “old” 70–55 Ma paleocanyon segment paralleling the Hurricane fault and an “intermediate” NW-flowing 25–15 Ma East Kaibab paleocanyon segment were linked together by the 5–6 Ma Colorado River as it was downwardly integrated from the Colorado Plateau to the Gulf of California. In this hypothesis, most of the Grand Canyon was incised by the Colorado River in the past 6 Ma. Karlstrom et al. (2017) reinforced this paleocanyon hypothesis and suggested that the 25–15 Ma East Kaibab paleocanyon was carved by an ancestral Little Colorado (not Colorado) River. Laramide (70–50 Ma) thermochronologic ages seen in many samples of that study were attributed to northward cliff retreat of Mesozoic strata off the Mogollon highlands rather than carving of a ~70 Ma Grand Canyon. Fox and Shuster (2014) proposed that thermochronologic data from the westernmost Grand Canyon were compatible with “young” incision provided that sufficient radiation damage was retained during burial, thereby effectively changing the predicted temperature sensitivity of the system at the time of canyon incision. However, interpretations of thermochronology data from the westernmost Grand Canyon segment remain in controversy (Flowers et al., 2015).

Here we applied the three different apatite thermochronology methods using apatite from the same sample from the westernmost Grand Canyon to resolve conflicting thermal histories generated by inverse modeling of different datasets originating from the same sample. Our key sample (sample #1; see Table 1) has new, high precision $^4\text{He}/^3\text{He}$ data, multiple AHe ages, and AFT data and is from the same location as the single Flowers and Farley (2012) $^4\text{He}/^3\text{He}$ sample (#2) upon which their “old” Canyon conclusion was mainly based. These are from Separation Canyon, RM 240, where RM = river miles downstream of Lees Ferry (Stevens, 1983). We also report two new samples with combined AFT and AHe data and two new samples with AFT data that span from RM 225–260. Our objective is to re-evaluate and reconcile all new and published thermochronologic data from the westernmost Grand Canyon including AFT and AHe from Lee et al. (2013), AHe from Flowers et al. (2008), and $^4\text{He}/^3\text{He}$ from Flowers and Farley (2012).

Westernmost Grand Canyon is defined as the segment between Diamond Creek (RM 225) and the Grand Wash Cliffs (RM 276) (Fig. 1). We use the term “old” Canyon for time–temperature (t – T) paths that have a single cooling pulse at 70–55 Ma during which rocks cool to <30 °C and hence to within ~200 m of river level using a 25 °C surface temperature and a 25 °C/km geothermal gradient (Wernicke, 2011). We use the term “young” Canyon for either

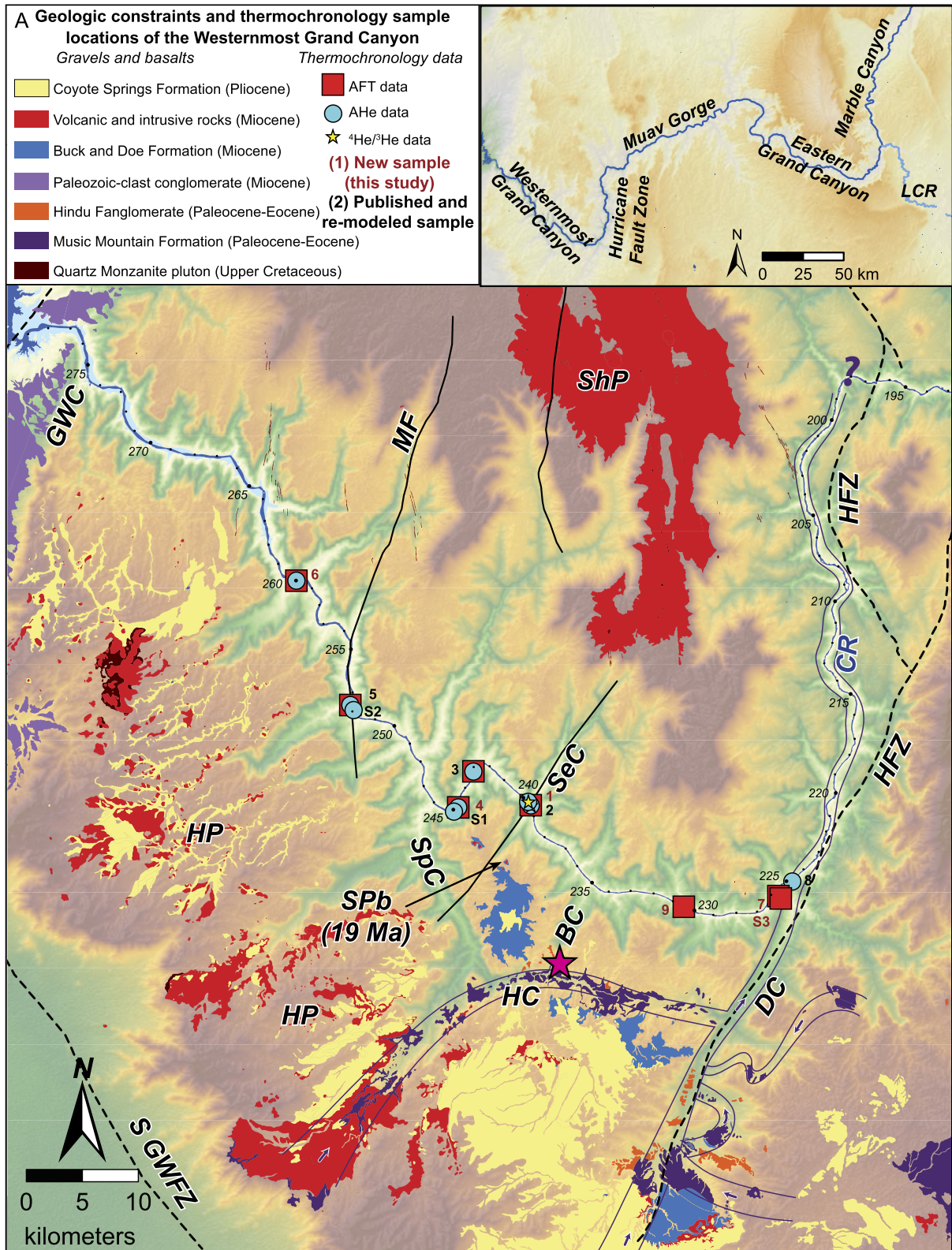


Fig. 1. A) Regional map showing geologic constraints and thermochronology sample locations in westernmost Grand Canyon and the extent of Tertiary gravels and volcanic deposits across the Hualapai Plateau, modified from Billingsley et al. (2006) and Karlstrom et al. (2014). Inset map shows sections of the Grand Canyon. Pink star is the location of north-derived key Hindu Fanglomerate exposure at head of Bridge Canyon. B) Google Earth image, looking SE, highlighting the incision surrounding the Separation Point Basalt (SPb) and its source flow. Geographic features are: BC = Bridge Canyon, CR = Colorado River, DC = Diamond Creek, GWFZ = Grand Wash fault zone, GWC = Grand Wash Cliffs, HC = Old Man-Hindu Canyon, HFZ = Hurricane fault zone, HP = Hualapai Plateau, MF = Meriwitica monocline and fault, PSC = Peach Springs Canyon, SeC = Separation Canyon, ShP = Shivwits Plateau, SpC = Spencer Canyon.

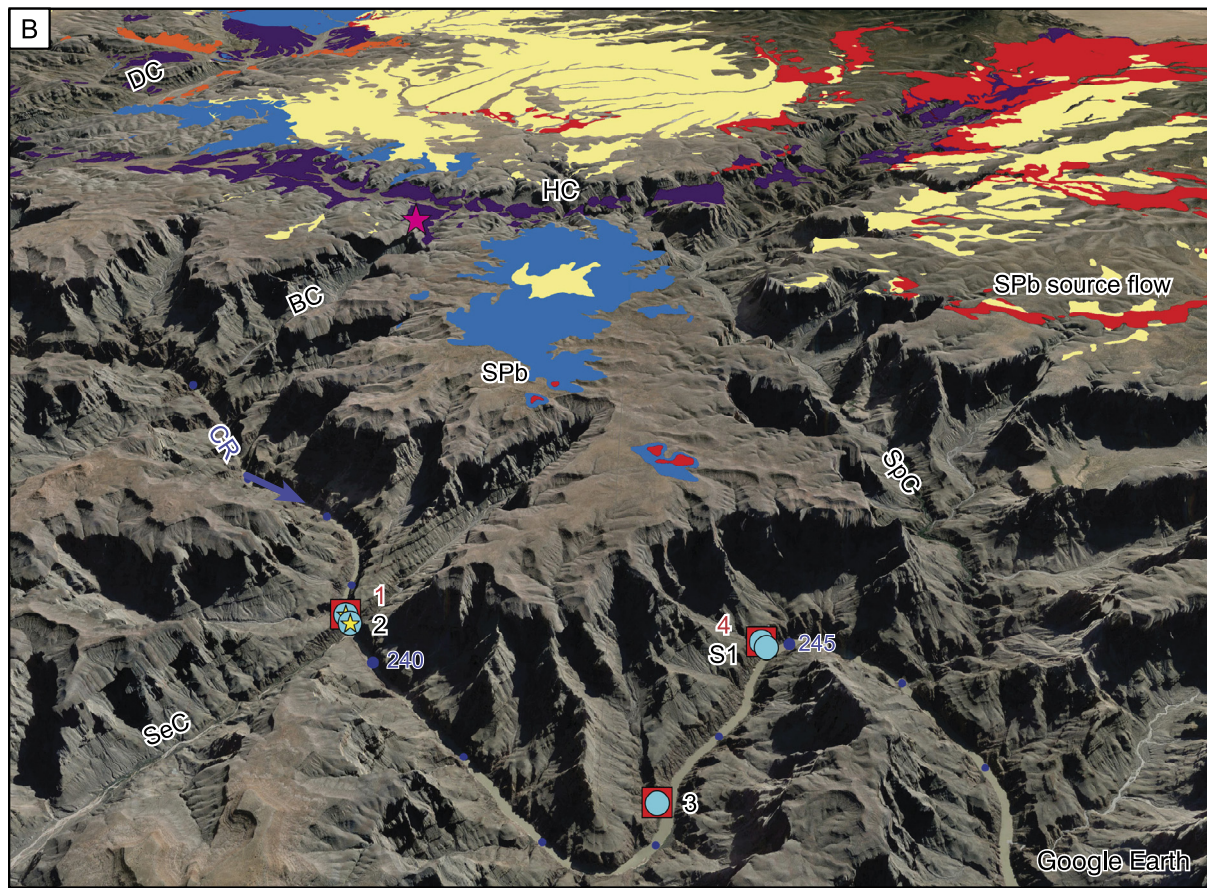


Fig. 1. (continued)

a single-stage cooling history that does not reach temperatures of $<30^{\circ}\text{C}$ by 50 Ma or a two-stage cooling history with cooling pulses at 70–50 Ma and at <6 Ma separated by a period of long-term residence at temperatures of $40\text{--}60^{\circ}\text{C}$. These temperatures correspond to burial by 0.8 to 1.4 km of sedimentary rock, the depth of the modern westernmost Grand Canyon measured from the south and north rims respectively, and indicate no westernmost Grand Canyon had been carved.

2. Summary of recent geologic studies supporting a <6 Ma westernmost Grand Canyon

Several recent studies have reinforced the evidence for a “young” 5–6 Ma westernmost Grand Canyon, independent of thermochronology-based studies. “Rim gravels” (e.g. Young, 2001) on the Hualapai Plateau (Fig. 1A) document an aggrading base level from 65–55 Ma (Music Mountain Formation), through ~ 24 Ma (Buck and Doe Formation), to younger than ~ 19 Ma (Coyote Springs Formation), aggradation which is incompatible with a deep paleocanyon of near-modern depth during this time (Young and Crow, 2014). The Paleocene Music Mountain Formation is interbedded with the Hindu Fan conglomerate (see star in Fig. 1A and 1B), which locally contains clasts sourced from the Kaibab escarpment to the north and precludes the presence of a paleo-Grand Canyon in the Eocene (Young and Crow, 2014). The 19 Ma Separation Point basalt (Wenrich et al., 1995) overlies the Buck and Doe Formation in a location on the Hualapai Plateau that has been steeply incised on all sides (Fig. 1B) suggesting lowering of base level after 19 Ma (Young and Crow, 2014).

Darling and Whipple (2015) examined the longitudinal profiles of Colorado River tributary drainages and compared them to profiles of similar-sized drainages established on the 17 Ma Grand

Wash escarpment. From this comparison, Darling and Whipple (2015) concluded that the morphology of the tributary drainages and slopes adjacent to the westernmost Grand Canyon must be younger than the 17 Ma Grand Wash escarpment. They also noted that the beveling of the Hualapai Plateau indiscriminately across lithologies is indicative of a long-lived base level incompatible with a long lived paleo-Grand Canyon. A third conclusion is that a 70 Ma westernmost Grand Canyon requires improbably low erosion rates of ~ 4 m/m.y. maintained for tens of millions of years.

The “Muddy Creek constraint” is based on sediments from Grand Wash Trough, at the mouth of the Grand Canyon, that contain limited or no Colorado Plateau detritus and no far-traveled gravels from a pre-6 Ma Colorado River; instead, this area was internally drained prior to 6 Ma (Longwell, 1946; Blackwelder, 1934; Lucchitta, 1966, 1972). More recent support for the Muddy Creek constraint comes from the geometry of the Miocene Pearce Canyon fan deposited across the modern path of the Colorado River (Lucchitta et al., 2013), and by detrital zircon data from siltstones near the mouth of the Grand Canyon that show no far-traveled sediment from the Colorado Plateau or Grand Canyon between 13 and 7 Ma (Crossey et al., 2015). Each of these lines of evidence refutes an “old” deeply carved canyon that followed the path of the westernmost Grand Canyon.

3. Procedures and parameters of thermochronologic modeling

Thermal history models were calculated incorporating data from multiple thermochronometers using HeFTy software (v. 1.8.3) (Ketchum, 2005), with constraints based on the best understanding of the geologic history of the sampled rocks (Fig. 2). We assumed a surface temperature of $20 \pm 10^{\circ}\text{C}$, which spans the range of surface temperatures assumed in published studies for this region. All

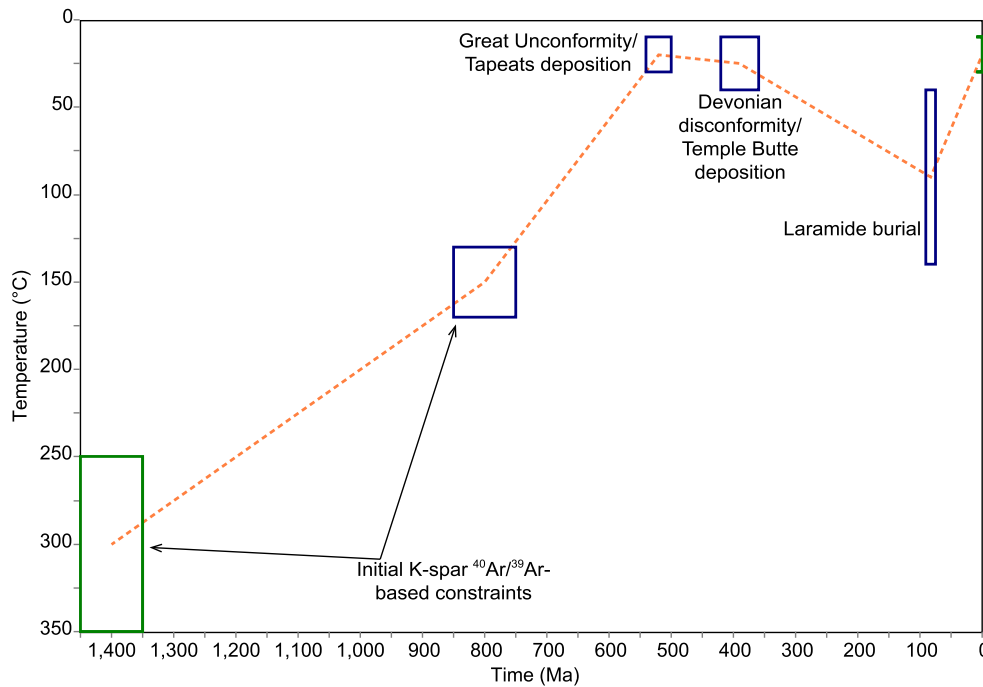


Fig. 2. Constraint boxes imposed on models (using HeFTy v. 1.8.3) for all samples and their geologic justifications. The long period of time that samples resided in and below the partial retention zone between Precambrian and Laramide times may have resulted in extensive radiation damage that was not fully annealed in the Laramide and hence produced complex and variable He diffusion behavior in apatite.

thermal models assumed the Radiation Damage Accumulation and Annealing Model (the RDAAM; Flowers et al., 2009), which quantifies He diffusivity in apatite through geologic time. The RDAAM accounts for the effects of radiation damage concentration on helium diffusivity in apatite (Shuster et al., 2006) by assuming the annealing behavior of fission tracks can be used as a proxy for alpha-recoil damage annealing (Flowers et al., 2009).

For many of our samples the ages appear to be over-dispersed (Vermeesch, 2010) and we were unable to find time–temperature paths that predict the observed AHe ages within error. The issue of age dispersion is a problem faced by other thermochronology studies (e.g. Vermeesch, 2010) that needs to be better addressed by the apatite thermochronology community. In our case, in order to attempt to account for over-dispersion, we increased the measured uncertainty proportionally until we were able to find time temperature paths that could explain the data, which is equivalent to lowering the p-value and accepting more paths (Vermeesch and Tian, 2014). Over-dispersed ages may arise because uncertainty in AHe ages is estimated using the high precision of the He, U and Th molar abundance measurements. These “analytical” uncertainties that do not incorporate additional uncertainties, such as: corrections for alpha ejection that do not account for the true shape of the crystal or the spatial distribution of U and Th (Ault and Flowers, 2012), possible undetected micro inclusions (Farley and Stockli, 2002), or neighboring minerals leading to alpha – injection (Spiegel et al., 2009). Therefore, the reported “analytical” error likely underestimates system uncertainties. Other assumptions in the models used to interpret the data may also not account for the true complexity of the system. For example, Cl content may control the temperature and rate of radiation damage annealing (Carlson et al., 1999; Donelick et al., 2005; Gautheron et al., 2013) and this is not accounted for in the RDAAM. Therefore, when discussing “good” and “acceptable” paths below, these are in relation to the data with additional uncertainty included that attempts to account for the over-dispersed ages. For complete transparency, a comparison of predicted ages and corrected ages are therefore shown for each model result figure.

Constraint boxes (Fig. 2) were defined by potassium feldspar $^{40}\text{Ar}/^{39}\text{Ar}$ thermochronology data from McDermott (2011) and the known geologic history of the region (DR-7). Because all apatites are from Proterozoic basement rocks near river level, t – T paths began during the Precambrian and cooled to near-surface temperatures by Cambrian time beneath the Great Unconformity, with depth of near-surface residence thereafter determined by deposition and erosion of Paleozoic (~ 1 km) and Mesozoic (~ 2 km) strata. Flowers and Farley (2012) modeling of AHe data assumed that apatites were completely reset, and radiation damage was annealed, at temperatures of 110–120 °C at 80–100 Ma, just before the Laramide orogeny, and therefore began their thermal history models at these t – T conditions. However, long-term low-temperature residence of apatites between the Cambrian and the Laramide in our modeling allows for extensive pre-Laramide accumulation of radiation damage, which may or may not have been completely annealed by Laramide burial (Fox and Shuster, 2014), and our broader 40–140 °C Laramide constraint box allow the data themselves to determine maximum Laramide burial temperatures.

In addition to reanalyzing the key sample (#2) from the Flowers and Farley (2012) study, we pursue a multi-sample approach to test geologic evidence for spatially variable thermal histories during progressive north-to-south cooling (Flowers et al., 2008) due to cliff retreat (Karlstrom et al., 2014, 2017), Laramide reverse and Miocene normal faulting (Huntoon et al., 1981, 1982), and the formation of older paleocanyon segments (Kelley et al., 2001; Young and Hartman, 2014; Karlstrom et al., 2014). These geologic factors argue against the assertion of Flowers et al. (2015) that “all western Grand Canyon samples have the same thermal history”. Instead, we consider samples and data types individually before synthesizing the thermochronology of westernmost Grand Canyon relative to the geologic evidence outlined above.

Throughout this paper, we assume average surface temperatures of 25 °C and a geothermal gradient of 25 °C/km (Wernicke, 2011). Estimates of the surface temperature for westernmost Grand Canyon range between 10–25 °C (average surface temperature in Death Valley is 25 °C), whereas geothermal gradient estimates are

Table 1
Summary of thermochronologic data modeled in this study.

Sample number	River mile	Sample ID	Data source	Source rock description (Karlstrom et al., 2003)	AHe age range (Ma)	eU range (ppm)	# of AHe ages	AFT age	AFT lengths
1	240	10GC161	<i>this study</i>	Separation pluton: weakly foliated, medium-grained granite; 1.71–1.68 Ga	55.3–93.4	1.1–14.6	4	60.8 ± 4.4	13.1 ± 1.6(102)
2	240	CP06–69	Flowers et al., 2008, 2012	Separation pluton: weakly foliated, medium-grained granite; 1.71–1.68 Ga	64–76	11–13	5	–	–
3	243	01GC86	Lee et al., 2013	245-mile pluton: weakly foliated granodiorite; 1.73 Ga	29–72	10.6–17.1	3	62.8 ± 4	13 ± 0.4(67)
4	245	10GC164	<i>this study</i>	245-mile pluton: weakly foliated granodiorite; 1.73 Ga	66.9–94.9	7.2–18.7	6	72.2 ± 5.9	13.1 ± 1.6(92)
S1	245	CP06–71A	Flowers et al., 2008	245-mile pluton: weakly foliated granodiorite; 1.73 Ga	48–55	5–14	4	–	–
5	252	01GC87	Lee et al., 2013	Surprise pluton: granite; 1.7 Ga	69.5–90.1	81.8–231.7	6	68.7 ± 3.8	12.1 ± 0.4(101)
S2	~ 252	GC863	Flowers and Farley, 2012	Surprise pluton: granite; 1.7 Ga	54–71	47–85	6	–	–
6	260	MH10–260	<i>this study</i>	Quartermaster pluton: megacrystic non-foliated granite; 1.35 Ga	15–71	3–34	4	63.2 ± 7	12.3 ± 2(5)
7	225	04GC138	<i>this study</i>	Diamond Creek pluton: granodiorite; 1.73 Ga	–	–	–	114 ± 6.5	13.3 ± 2.4(66)
S3	225	04GC139	<i>this study</i>	Diamond Creek pluton: granodiorite; 1.73 Ga	–	–	–	112 ± 6.1	13.6 ± 2.2(47)
8	225	CP06–65	Flowers et al., 2008	Diamond Creek pluton: granodiorite; 1.73 Ga	51–81.4	32–48	4	–	–
9	230.5	MH10–230.5	<i>this study</i>	Travertine Falls pluton: medium-grained granite; 1.7 Ga	–	–	–	69.0 ± 6.2	12.8 ± 2.1(101)

between 18–30 °C/km; these estimates are generally based on well log and heat flow data summarized by Wernicke (2011). The assumptions of Wernicke (2011) and Flowers and Farley (2012) provide a reasonable ‘minimum’ value for a paleodepth estimate given the relatively high surface temperature estimate. However, these assumptions regarding the inversion of temperature to burial depth represent a major uncertainty in any thermochronologic study that involves estimating burial depth from temperature. These values undoubtedly vary by location and through geologic time in ways that are not quantifiable. Variables that have undetermined effects on surface temperatures and geothermal gradients through time and space include changes in the climate, elevation, and mantle temperatures; variations in thermal conductivity as strata are deposited and eroded; and the transient flow of groundwater. Complexities of how isotherms mimic topography in cases of ragged cliff retreat and/or below the edge of Music Mountain paleovalleys may also result in variations in the geothermal gradient. Thus, given the wide variation in published surface temperature and geothermal gradient assumptions compiled in Supplementary Table 2 of Karlstrom et al. (2014), thermochronology-determined paleodepths remain approximate and represent a continued uncertainty in geologic interpretations of thermal history models. While it is worth acknowledging these variables as a major uncertainty in our depth estimates, it is beyond the scope of this paper to attempt to quantify the many effects of these variables. For the purposes of

this study, it is enough to recognize that for a t - T path to be compatible with the proposed model of an “old” westernmost Grand Canyon cut to within 200 m of its modern depth (Wernicke, 2011), t - T paths must reach ~30 °C by 70–50 Ma, using the above assumptions. In contrast, modeled temperatures of ~40 °C are interpreted to reflect ~600 m burial, the elevation differential between the river and present south rim in the westernmost Grand Canyon. Use of any higher geotherm or lower average surface temperature increases the interpreted depth of burial.

4. New thermochronologic data and thermal history models

All new and some previously published data used in this study are reported in the supplementary files and data repository of this paper. New AFT ages and lengths are presented in DR-1. Chemical data indicate that apatites from the westernmost Grand Canyon are dominantly fluoro-apatite, with low concentrations of Cl, indicating relatively rapid annealing of fission tracks. DR-2 presents new $^4\text{He}/^3\text{He}$ data, DR-3 presents published AHe data with errors and uncorrected ages (back-calculated in the case of Lee et al., 2013), DR-4 presents new AHe data, and DR-5 presents all goodness-of-fit (GOF) data and modeling parameters used for the thermal history models done in this study. Supplementary figures, including modeled thermal histories of published AHe data, are shown in DR-6

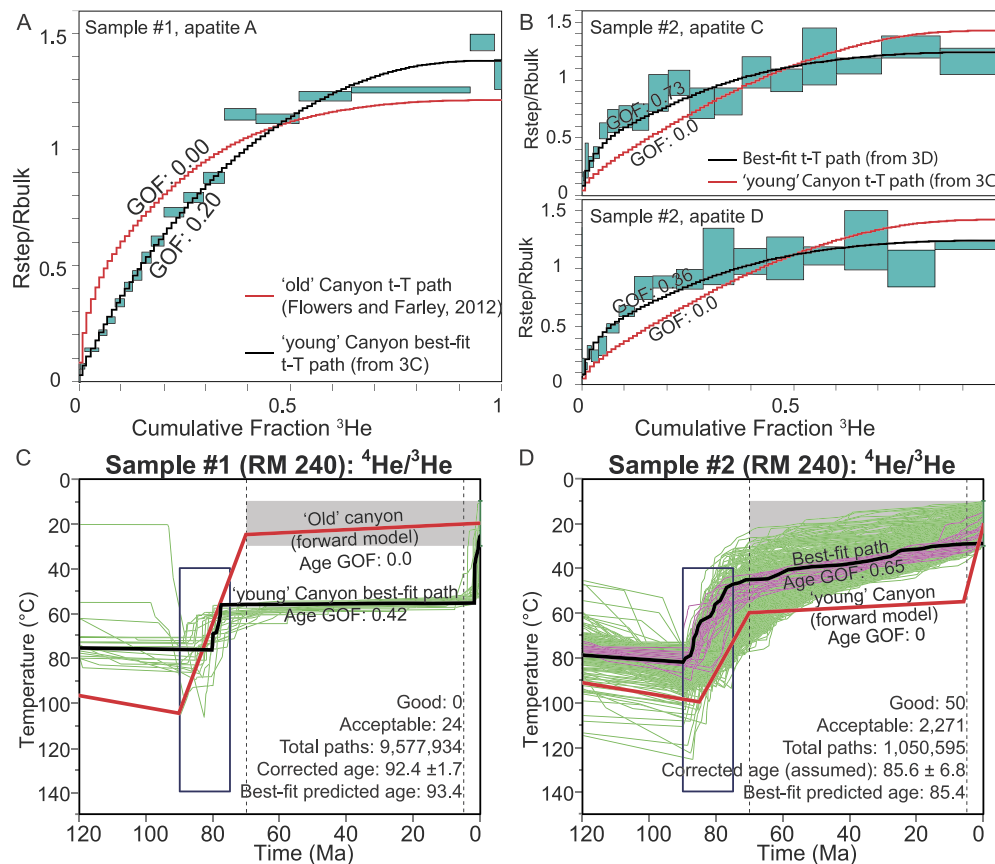


Fig. 3. New and previously published $^4\text{He}/^3\text{He}$ data from sample #1 (this paper) and #2 (Flowers and Farley, 2012) from the same location at Separation Canyon. A) New data (sample #1) are more precise than prior data (#2) and are best predicted by the “young” Canyon t - T path shown in black. B) Flowers and Farley (2012) data as modeled in this paper are also best predicted by a “young” Canyon. C) Inverse thermal history model of apatite A from sample #1, using the measured age of this grain (93.4 Ma) and assuming no zonation, returned a tightly constrained “young” Canyon thermal history shown in black. D) Inverse thermal history model of the Flowers and Farley (2012) data using the same AHe age and error that they used; note that the ages for apatites C and D were not measured but were based on the mean AHe age (85.6 ± 6.8 Ma) and eU (12 ppm) from other AHe analyses for this sample (Flowers et al., 2008). The good and best-fit paths support a “young” Canyon for both samples, but paths reside at $\sim 40^\circ\text{C}$ (#2) instead of 50 – 60°C (#1). (For interpretation of the references to color in this figure, the reader is referred to the web version of this article.)

and a detailed summary of methodology and model results is presented in DR-7.

Each of the t - T path diagrams generated using HeFTy software shows the imposed t - T constraint boxes that are based on geologic observations, the good and/or acceptable t - T paths, and a gray bar that indicates the range of surface temperatures that need to be reached by 50 Ma to support the “old” Canyon hypothesis. “Good” paths are designated by a goodness-of-fit (GOF) of $p = 0.5$ or greater and are shown in pink, while “acceptable” paths have a GOF of $0.05 < p < 0.5$ and are shown in green, where p is the probability that the chosen path could represent the data in question. Per the user manual for HeFTy v.1.8.3, the relative statistical fitting of good vs. acceptable paths implies that a “good” t - T path is supported by the data, while an “acceptable” t - T path is not ruled out by the data.

4.1. Sample #1, Separation Canyon (RM 240): Combined AFT, AHe, and $^4\text{He}/^3\text{He}$ data

Sample #1 (10GC161) is a new sample collected in the same location as sample #2 (CP06–69) from Flowers et al. (2008) and Flowers and Farley (2012), which was the single key sample with interpretable $^4\text{He}/^3\text{He}$ and AHe data that led to their “old” Canyon conclusion. We applied all three complementary apatite thermochronology methods to this new sample. This section highlights initial inconsistencies in t - T paths derived from different thermochronologic data types in this location and throughout the westernmost Grand Canyon. Thermal history modeling was initially

unable to produce any good or acceptable t - T paths when all three datasets (AHe, AFT, and $^4\text{He}/^3\text{He}$) were combined after $\sim 500,000$ random paths for sample #1 (10GC161). Thus, we modeled the datasets independently (Fig. 3 and Supplementary Fig. 1) to generate viable t - T paths and then compared these t - T paths for both sample #1 and sample #2 (Fig. 4A). Our reconciliation of all data into a single thermal history by modifying modeling parameters is presented after an exploration of the separate datasets.

Bulk AHe ages for both sample #1 and #2 (age range 55.3–93.4 Ma and 64–76 Ma, respectively; Table 1), considered on their own, can be predicted by “old” Canyon t - T paths that cool in a single event to near surface temperatures ($\sim 30^\circ\text{C}$) by ~ 70 Ma, in apparent agreement with Flowers and Farley (2012). AFT data from sample #1 (age of 60.8 Ma) are best predicted by t - T paths that cool gradually from peak Laramide temperatures of 100 – 140°C to reach surface temperatures after 20 Ma and prefer a “young” Canyon (DR-6, Supplementary Fig. 1). However, even with track length data, these AFT data alone are relatively insensitive to the $< 60^\circ\text{C}$ part of the t - T path where the controversy lies.

Fig. 3 shows high-precision $^4\text{He}/^3\text{He}$ data obtained from sample #1, apatite A (Fig. 3A), and our new model of $^4\text{He}/^3\text{He}$ data from sample #2 using our constraint boxes and the published U and Th zonation profiles for apatites C and D as model inputs (Fig. 3B). The increased precision of $^4\text{He}/^3\text{He}$ data from sample #1 is due to higher ^4He concentration, derived from both larger crystal size and slightly higher U and Th concentrations. Accurate $^4\text{He}/^3\text{He}$ modeling requires knowledge of both the measured age and the U and

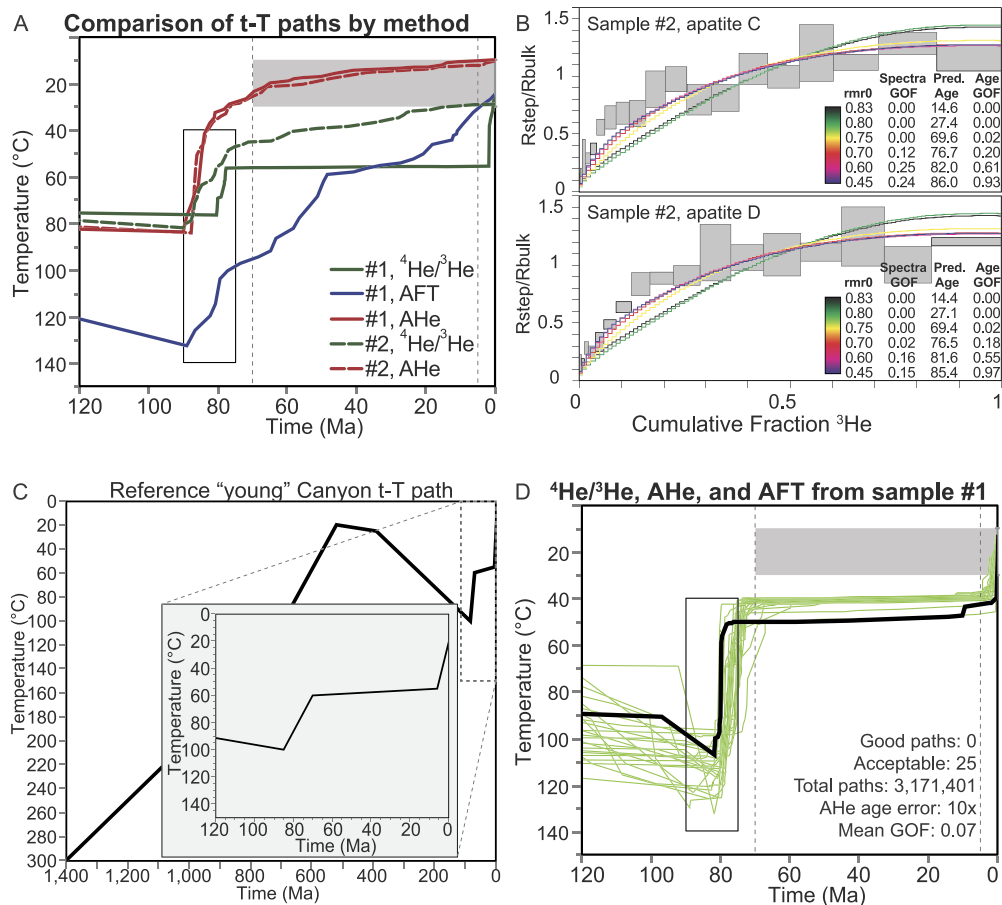


Fig. 4. Reconciling the disagreement between Separation Canyon t - T paths. A) Best-fit t - T paths from different analysis methods and samples (Sup. Fig. 1, Fig. 3) from the same location at Separation Canyon show marked disagreement when modeled separately. B) To reconcile data, we adjust the r_{mr0} value (a proxy for grain retentivity) in RDAAM using data from Flowers and Farley (2012) to test a "young" Canyon reference path and find that assuming higher grain retentivity by decreasing the r_{mr0} values to 0.6–0.45 (red and blue curves) predicts the $^4\text{He}/^3\text{He}$ data with an acceptable GOF of 0.55–0.97, respectively. C) Reference "young" Canyon path used in B for varying r_{mr0} ; inset of C shows blow up of the forward model after 120 Ma, the time of interest for this study. D) By adjusting r_{mr0} values (different amounts for different samples, see Supplementary data), RDAAM was able to predict all datasets together to return a suite of acceptable t - T paths that reside at 40–50 °C after 70 Ma and reach surface temperatures after 5 Ma. For GOF figures associated with this model, readers are referred to DR-6, Supplementary Fig. 5. (For interpretation of the references to color in this figure legend, the reader is referred to the web version of this article.)

The zonation profile of an apatite crystal; unfortunately only one or the other can be measured on the same crystal as a consequence of the destructive nature of each measurement. Flowers and Farley (2012) measured zonation for sample #2 and used an assumed age of ~85 Ma (corrected) based on the mean age of four other apatite grains in the sample that had been previously analyzed (Flowers et al., 2008). Conversely, we measured the age of apatite A of sample #1 (93.4 Ma, corrected) and assumed no zonation in our modeling of this data, based on minimal zonation present in other crystals from this rock seen in the distribution of fission tracks and further analysis in the companion paper (Fox et al., 2017; see Supplementary Fig. 2 and Flowers and Farley, 2012).

$^4\text{He}/^3\text{He}$ data for sample #1 are best predicted by "young" Canyon t - T paths shown in Fig. 3A and 3C. These paths show two-stage cooling: from 75 °C to ~60 °C at ~80 Ma, long-term residence at ~55 °C, and then cooling to surface temperatures after 5 Ma. For comparison, an approximate 'old' Canyon path from Flowers and Farley (2012) (red lines in Figs. 3A and 3C), does not predict the new $^4\text{He}/^3\text{He}$ data in Fig. 3A. These new data alone therefore provide strong support for a "young" Canyon.

Fig. 3D shows our new inverse modeling of sample #2 with $^4\text{He}/^3\text{He}$ data for two grains (C and D) using our constraint boxes that represent the complete thermal history and do not assume full annealing in the Laramide. The data are best predicted by t - T paths that reside at ~40 °C after the Laramide, although cooling

still appears to be single-stage. We still interpret this as favoring a "young" Canyon because a temperature of 40 °C corresponds to a minimum of 600 m of burial assuming a 25 °C surface temperature and 25 °C/km geothermal gradient, and does not support an "old" Canyon carved to within 200 m of the modern depth at this location. Thus, both samples #1 and #2, when modeled using $^4\text{He}/^3\text{He}$ alone, favor a "young" Canyon and the uncertainty is whether rocks resided at ~55 °C (1.2 km) or ~40 °C (0.6 km) using the minimal depth conversion values of 25 °C and 25 °C/km.

Fig. 4A shows a summary of the best-fit paths for samples #1 and #2 generated by independent modeling of the three types of datasets (AHe, AFT, and $^4\text{He}/^3\text{He}$) from the Separation Canyon location. Best-fit t - T paths from AHe data for both samples favor an "old" Canyon and are in striking disagreement with the thermal histories that best predict the $^4\text{He}/^3\text{He}$ data. Paths from the $^4\text{He}/^3\text{He}$ data and AFT data from sample #1 differ, but overlap near 50–60 Ma, the AFT age of this sample. For the Separation Canyon location, AFT and $^4\text{He}/^3\text{He}$ data, when modeled individually, are compatible with post-Laramide residence temperatures of 40–60 °C and a "young" Canyon whereas the t - T paths for the AHe data cool to near-surface temperatures by 70 Ma and are compatible with an "old" Canyon.

The importance of applying all methods to the same sample and of comparing different datasets from the same location is that it highlights inconsistencies between predicted t - T paths and re-

veals a significant error in the model. It is physically impossible for these apatites to have undergone different cooling histories. Our approach to reconcile all of the datasets is to favor the AFT and $^4\text{He}/^3\text{He}$ data, which agree best with the geologic evidence outlined earlier in this paper and provide better constraints on thermal history solutions due to the greater number of data in these measurements. For westernmost Grand Canyon, where the discussion is focused on the lowest temperatures of apatite sensitivity, AHe ages alone have limited resolution in comparison to $^4\text{He}/^3\text{He}$. $^4\text{He}/^3\text{He}$ data is also internally consistent as it originates from a single crystal, and is consequently subject to fewer variables and less uncertainty within the RDAAM. AHe ages from multiple crystals may be influenced by varying parameters per crystal that affect He diffusion kinetics (such as Cl content) that may not be accounted for by the RDAAM and therefore may not accurately predict the independent evolution of each crystal.

To account for uncertainty in the rate of alpha-recoil damage annealing, and its influence on He diffusivity, we adjust the $r_{\text{mr}0}$ parameter in the RDAAM, following Fox and Shuster (2014). This empirically derived parameter links AFT annealing to alpha-recoil damage annealing and reflects the grain's resistance to annealing of radiation damage, which strongly influences He retentivity after reheating during sedimentary burial. Lower $r_{\text{mr}0}$ values represent more retentive apatite that has a higher closure temperature range (Gautheron et al., 2013); thus AHe ages with lower $r_{\text{mr}0}$ values are best predicted by higher temperature t - T paths. The RDAAM assumes a value of 0.83, which represents a typical fluorapatite's resistance to annealing; however values generally range between zero and one, with most values between 0.65 and 0.85, and often vary from apatite to apatite (Carlson et al., 1999; Ketchum et al., 1999; Ketchum et al., 2007). Fig. 4B shows the effect of lowering $r_{\text{mr}0}$ from the default value of 0.83 to 0.60 for a reference "young" Canyon path (Fig. 4C) for the $^4\text{He}/^3\text{He}$ spectra of sample #2. Lowering $r_{\text{mr}0}$ to 0.60 increases the GOF from 0.0 to 0.25 for grain c and from 0.0 to 0.16 for grain d. This point was also made by Fox and Shuster (2014) using a different modeling approach.

Fig. 4D shows that all three datasets in sample #1 (AHe, AFT, and $^4\text{He}/^3\text{He}$) can be predicted by the same "young" Canyon t - T paths by adjusting the $r_{\text{mr}0}$ values of individual AHe ages. This required adjustment of the $r_{\text{mr}0}$ values for AHe ages and relaxing the age uncertainties to $10\times$ the analytical error allowed the AHe ages, AFT age and lengths, and $^4\text{He}/^3\text{He}$ data to be jointly modeled via the RDAAM, albeit with a poor GOF of 0.07. One AHe age (apatite X) was excluded from this model as an old outlier on a positive age-eU trend given by the other apatites Z, Y, and A (Supplemental Fig. 1B). The t - T path from this final combined dataset (Fig. 4D) shows a narrow set of 25 acceptable GOF paths after over 3 million total paths were tested. These paths were only generated by varying $r_{\text{mr}0}$ values for the different apatites to 0.70, 0.60, and 0.60 for apatites A (with $^4\text{He}/^3\text{He}$ data), Z, and Y respectively. Other values for $r_{\text{mr}0}$ for apatite A were tried, but resulted in unrealistic values of $r_{\text{mr}0}$ values (0.20 and lower) for the other two apatites in order for t - T paths with acceptable GOF to be generated. Thus, our preferred thermal history for sample #1 and the Separation Canyon location reaches burial temperatures of 90–120 °C during the Laramide, cools rapidly to residence temperatures of 40–50 °C, and reaches surface temperatures after 5 Ma.

4.2. Combined (U-Th)/He and AFT models

This section expands the thermochronologic coverage to other areas of the westernmost Grand Canyon with the samples listed by river mile in Table 1. We present new modeling of previously published samples from Lee et al. (2013): sample #3 (01GC86, RM 243) and #5 (01GC87, RM 252) using our uniform model constraint

boxes and new chemical data for the AFT analyses. We also report new combined AFT and AHe analyses for sample #4 (10GC164, RM 245) and #6 (MH10–260, RM 260). Thermal histories for the jointly modeled datasets are presented in Fig. 5A–D.

4.2.1. Sample #3 (01GC86, RM 243); 245-mile granodiorite

Fig. 5A shows t - T paths that predict the combined AFT and AHe data from sample #3 (01GC86) from Lee et al. (2013). Three AHe ages range from 29–72 Ma, with a scattered age-eU plot. Flowers et al. (2015) stated that this sample was "a problematic sample" because of high dispersion of ages and a younger mean age (50 Ma) than other samples in the western Grand Canyon and therefore should not be used for inverse modeling. In contrast, we see no reason to reject this analysis as similar ages are found in several other samples and we have accounted for unknown kinetic controls by increasing the estimated error for each age to achieve acceptable t - T paths using the RDAAM. Our preferred best-fit path shows a single cooling episode to ~ 40 °C by 40–50 Ma from burial temperatures of 90–130 °C during the Laramide and cooling to near-surface temperatures after ~ 20 Ma, similar to other thermal histories in this area. The thermal history generated by modeling the three AHe ages alone for this sample without the AFT data remain hotter, at ~ 70 °C, until after 20–30 Ma, when they cool to near-surface temperatures (Supplementary Fig. 3A). In this case, the addition of AFT to the AHe changes the modeled thermal history for this sample from a "young" Canyon path to closer to an "old" Canyon path, although neither path reaches near surface temperatures until after 20–30 Ma.

4.2.2. Sample #4 (10GC164, RM 245); Spencer Canyon pluton

Fig. 5B shows our preferred t - T path for the combined AFT and AHe data (5/6 grains) for sample #4, which is at the same location as sample #S1 (CP06-71A from Flowers et al., 2008; Supplementary Fig. 4A). The AFT age for sample #4 is 72.2 ± 5.9 Ma while the AHe ages range from 66.9–94.6 Ma. HeFTy generated acceptable t - T paths only after the age error was increased to 8x the analytical error. The best fit t - T path shows 100 °C peak burial temperatures during the Laramide followed by cooling to ~ 40 °C by 60 Ma and no second stage cooling. The model using AHe data alone for this sample (Supplementary Fig. 3B) shows a different t - T path using 3x the analytical error. These paths have a single stage of cooling from ~ 80 °C during the Laramide to near surface temperatures of 20 °C, compatible with an "old" Canyon. Thus, the AHe data alone predict an "old" Canyon whereas the combined AFT and AHe t - T paths are not compatible with an "old" Canyon because near-surface temperatures are not reached until after 20 Ma.

4.2.3. Sample #5 (01GC87, RM 252); Surprise Canyon pluton

Fig. 5C shows our preferred thermal history for this sample from Lee et al. (2013), which is at the same location as sample #S2 (GC863 from Flowers and Farley, 2012; Supplementary Fig. 4B). Six AHe ages range from 69.5–90.1 Ma with a generally positive age-eU slope; the AFT age is 68.7 ± 3.8 Ma. The combined datasets are best predicted by a t - T path showing a period of rapid cooling from ~ 90 °C to ~ 60 °C during the Laramide, mid-Tertiary slow cooling from 70 to 50 °C, and cooling to surface temperatures after 20 Ma. This suggests ~ 1.4 km of burial after the Laramide and favors a "young" Canyon. AHe data modeled alone (Supplementary Fig. 3C) return a poorly constrained swath of t - T paths that in general show cooling from 90–100 °C to ~ 40 °C during the Laramide before cooling gradually to surface temperatures, also favoring a "young" Canyon.

4.2.4. Sample #6 (MH10-260, RM 260); Quartermaster pluton

Fig. 5D shows our preferred t - T path for this sample generated with combined AFT and AHe data. The AFT age is 63.2 ± 7 Ma

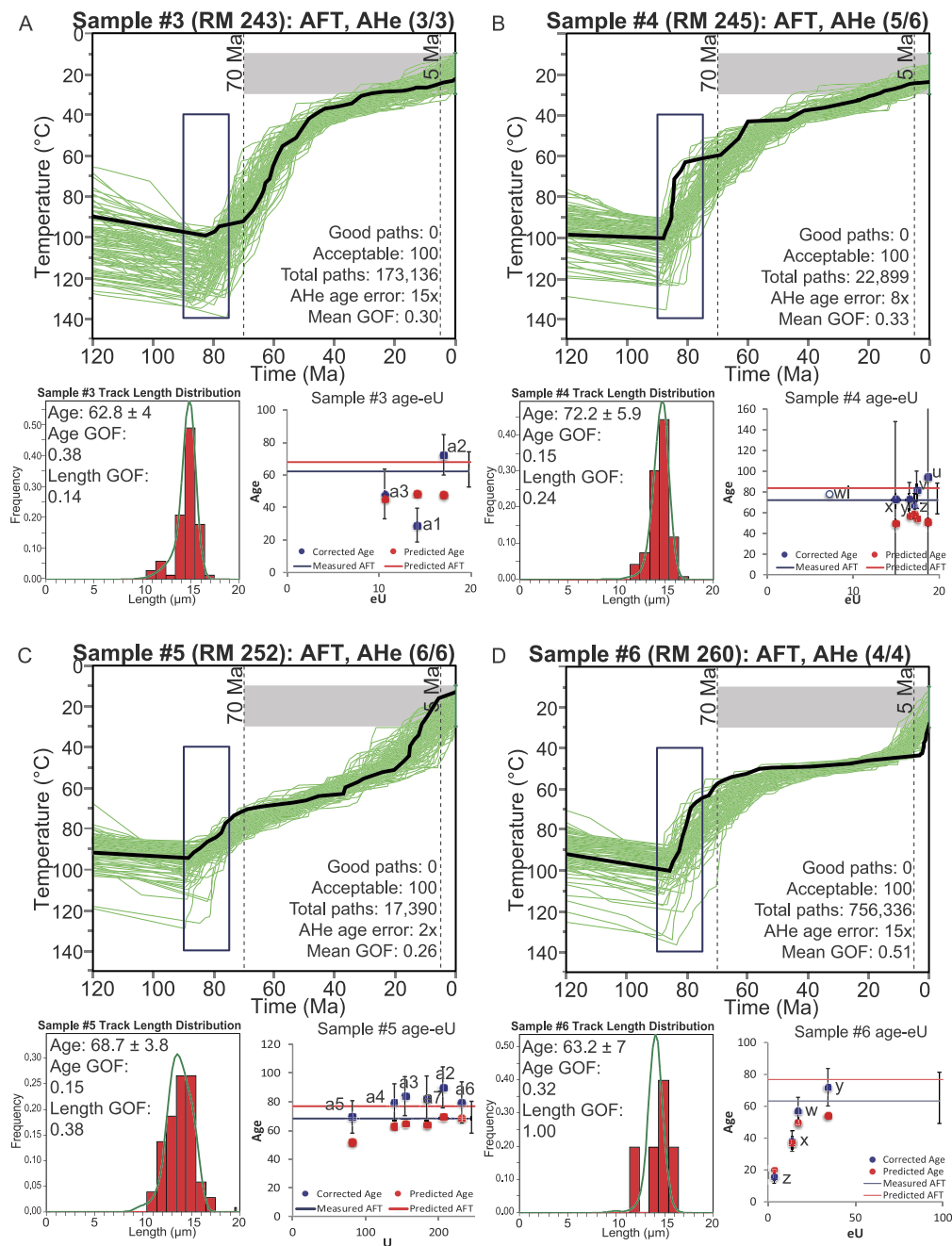


Fig. 5. Samples with combined AFT and AHe data; age-eU plots and AFT track length GOF are shown for each sample. A) Data from sample #3 are best predicted by a t - T path that cools to $\sim 40^\circ\text{C}$ during the Laramide. B) Data from sample #4 follow a similar cooling path as sample #3, but are slightly warmer after the Laramide. C) Data from sample #5 have a 2-stage cooling history; these paths stay at high temperatures ($\sim 60^\circ\text{C}$) after slight cooling during the Laramide and reach surface temperatures after 20 Ma. D) Data from sample #6 share a similar t - T path with #5, but reside at $\sim 50^\circ\text{C}$ and reach surface temperatures after 10 Ma.

and four AHe ages range from 15–71 Ma with a strongly positive age-eU slope. This model generated acceptable GOF paths only after relaxing the estimated errors to 15 \times the reported analytical uncertainties. The best-fit path has a two-stage cooling history that reaches a maximum burial temperature of $\sim 100^\circ\text{C}$ in the Laramide, cools between 85 and 70 Ma, and resides at $\sim 50^\circ\text{C}$ through 70–10 Ma. The inflection showing onset of young cooling takes place after about 5 Ma. Similar thermal history models are generated by jointly modeling the 4 AHe analyses without the AFT data (Supplementary Fig. 3D). The AHe t - T paths reach a slightly lower maximum burial temperature of $\sim 80^\circ\text{C}$ during the Laramide, cool and reside at $\sim 60^\circ\text{C}$, and then reach surface temperatures after 10 Ma. Thermal histories for both the combined datasets and the AHe data alone support a “young” Canyon in that

rocks remained at 50 – 60°C until after 10 Ma, suggesting a minimum depth estimate of ~ 1 km.

4.3. Samples #7 and #8 from Diamond Creek: proof of concept for the paleocanyon hypothesis

The above data from westernmost Grand Canyon show that the combined thermochronologic data of $^4\text{He}/^3\text{He}$ (2 samples), AHe ages (6 samples) and apatite fission-track analyses (5 samples) are best predicted by t - T paths compatible with a “young” Canyon. The “old” Canyon hypothesis, which predicts cooling to within 200 m of the surface (30°C) by 50 Ma, can be compatible with individual datasets but is not compatible with multi-method analyses from any of the samples. Consequently, the westernmost Grand

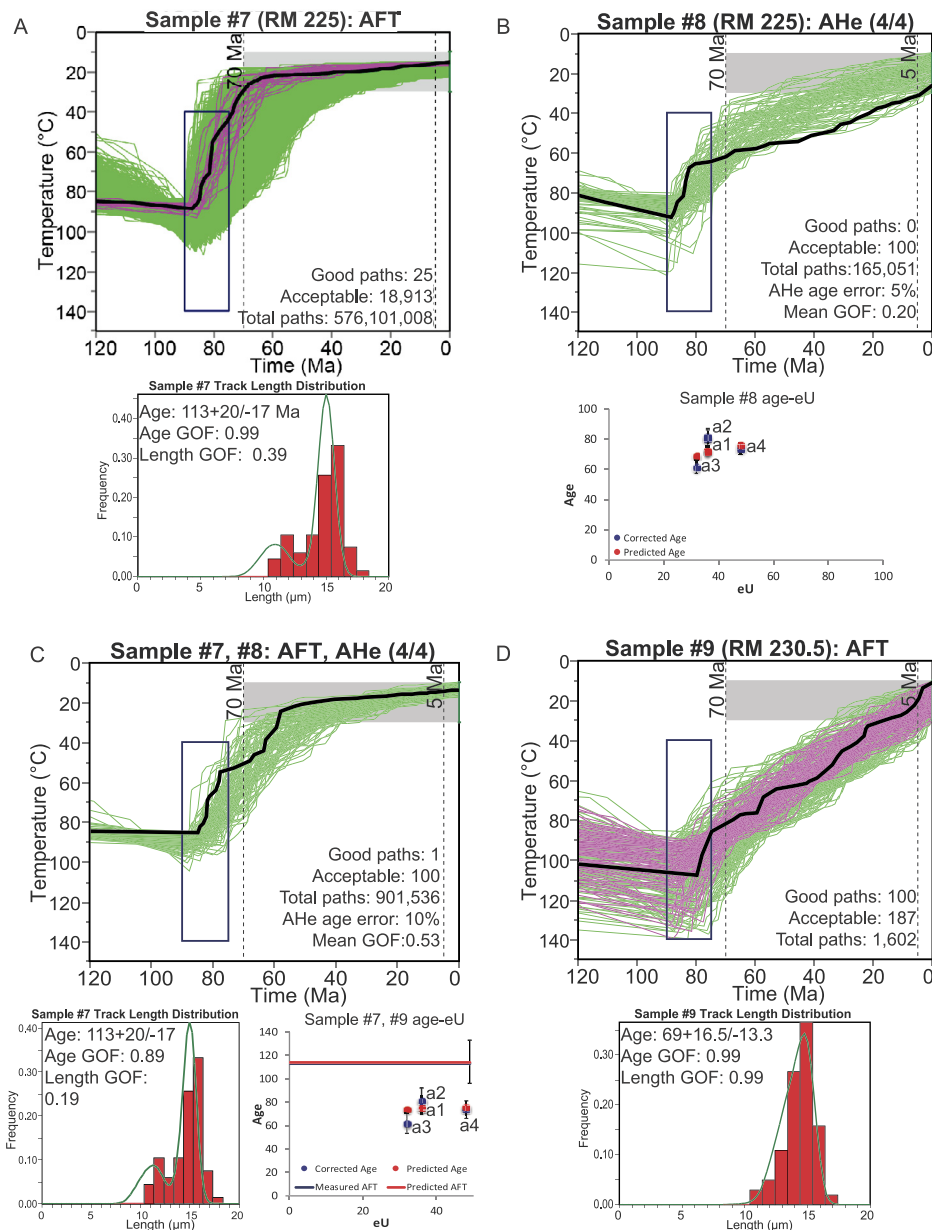


Fig. 6. The paleocanyon hypothesis of [Karlstrom et al. \(2014\)](#) suggests that samples from Diamond Creek, because they are in the Hurricane segment, should give “old” Canyon t - T paths. A) New sample (#7) from the same location as a key sample from [Kelley et al. \(2001\)](#) where AFT data are best predicted by an “old” Canyon t - T path, consistent with this segment having been carved by the ~55–65 Ma Music Mountain Formation system. B) Previously published AHe data from [Flowers et al. \(2008\)](#) from the same location as #7 that are best predicted by a “young” Canyon t - T path. C) Combining our AFT (sample 7) with AHe data from sample #8 yields t - T paths that reach surface temperatures by 60 Ma, compatible with the existence of a Music Mountain paleocanyon. D) New AFT data from river mile 230.5 are best predicted by a “young” Canyon t - T path. Note the significant difference between t - T paths from this sample (#9) and sample #7.

Canyon is a “young” segment, carved in its present position in the past 5 Ma.

To test whether any segments of Grand Canyon are “old” as proposed by [Karlstrom et al., 2014](#), we analyzed samples #7 (04GC138) and #S3 (04GC139) from Diamond Creek at RM 225 using AFT analysis. Diamond Creek is a tributary to the Colorado River ([Fig. 1](#)) where outcrops of the 55–65 Ma Music Mountain Formation occur at relatively low elevations and [Karlstrom et al. \(2014\)](#) and others ([Young, 2001](#); [Young and Hartman, 2014](#)) have proposed that a ~60 Ma N-flowing Paleocene river followed the Hurricane fault system. These samples are located near each other (within 60 m) with minimal elevation difference, and were collected near river level from the Diamond Creek pluton, at a similar location as sample #8 (CP06-65) from [Flowers et al. \(2008\)](#). If the paleocanyon hypothesis of [Karlstrom et al. \(2014\)](#) is correct, these

samples represent an important proof-of-concept via their comparison to the westernmost Grand Canyon and should have an “old” Canyon thermal history. Sample #7 (04GC138) has detailed Cl wt% and more track length measurements than sample #S3 (04GC139) and they are near enough to each other that a similar thermal history is required, so only sample #7 was modeled although data from both are presented in the data repository. The AFT age for sample #7 is 114.0 ± 6.5 , older than the AFT ages for all other samples considered in this study. High uranium rims are common in the analyzed apatites indicating some zonation. [Fig. 6A](#) shows that AFT data for sample #7 are predicted by a narrow suite of good GOF t - T paths that cool from ~90°C to surface temperatures by ~70 Ma. This single-stage cooling to surface temperatures supports that an “old” ~60 Ma paleocanyon was present at this location, but based on comparison with the westernmost Grand

Canyon data it was the northern extension of the Music Mountain paleoriver system and not carved by a paleo-Colorado River. Further support of low peak burial temperatures in this region comes from the bimodal peak of AFT track lengths in Fig. 6A and 6C.

Sample #8 (CP06-65) is a previously published sample from Flowers et al. (2008). This sample is also from the Diamond Creek pluton at the same location near RM 225. Fig. 6B shows that all AHe ages from sample #8 can be predicted by t - T paths that cool rapidly from 80–100 °C in the Laramide to temperatures of 30–60 °C before cooling gradually to reach surface temperatures throughout the Cenozoic, a single-stage cooling history that prefers a “young” Canyon at this location but does not preclude an “old” Canyon.

Fig. 6C shows t - T paths that combine AHe ages from sample #8 with AFT data from sample #7. Both are from the same location and must have had the same cooling history. Predicted ages in the age- eU plot for this combined data thermal history model are much better behaved than any other set of combined data in this region; the AFT age is significantly older than the AHe ages and therefore can be accurately predicted by the RDAAM. The t - T paths that result show a single stage of cooling in the Laramide, between 80 and 60 Ma, with rocks reaching about 30 °C by 60 Ma, compatible with an “old” Canyon. For comparison, Fig. 6D shows t - T paths that predict AFT data from sample #9 (MH10-230.5, this study). The AFT age for sample #9 is 69.0 ± 6.2 Ma, similar to other AFT ages in the westernmost Grand Canyon but much younger than the AFT ages for samples 7 and S3 at Diamond Creek. Sample #9's AFT t - T paths cool gradually from peak temperatures of 90–140 °C during the Laramide over the entire Cenozoic and reach surface temperatures after 20 Ma, compatible with a “young” Canyon.

5. Discussion: reconciling dataset inconsistencies

Fig. 7 takes the weighted mean t - T paths from different samples and analytical methods in order to compare modeling results. The results of the new analyses and new modeling using uniform geologic constraints back to the Precambrian show that a preponderance of these thermal histories, especially those that include combined datasets, support a “young” westernmost Grand Canyon (yellow envelope). Four thermal histories constrained by AHe data alone are best predicted by an “old” Canyon in Fig. 7 but these paths are discordant relative to all other paths, including paths from the same sample generated when the AHe data are integrated with $^4\text{He}/^3\text{He}$ and/or AFT data from the same samples and same locations. These disparate “old” and “young” Canyon t - T paths cannot both be geologically correct and must result from limitations of the thermal history modeling; i.e. assumptions within the most current model of apatite thermochronology systems behavior (the RDAAM) must not account for important variables in an area of low-temperature burial reheating such as the westernmost Grand Canyon.

In order to reconcile these discordant “old” Canyon AHe-only paths with the multi-dataset “young” Canyon paths and the geologic data, we varied the value of r_{mr0} in the RDAAM. The default value for the r_{mr0} parameter in the RDAAM assumes that alpha-recoil radiation damage anneals at the same rate as fission track damage for a specific temperature. By decreasing r_{mr0} within the range of its uncertainty (Ketcham et al., 2007), we assume that the rate of annealing alpha-recoil damage is somewhat lower than fission track annealing in apatite (as supported empirically; Ritter and Märk, 1986), which effectively increases the He retentivity of each apatite grain after burial heating (Fox and Shuster, 2014). Since Laramide burial depths and resulting temperatures (75–140 °C based on t - T paths from this study) may not have been sufficiently high enough or endured for a sufficient time

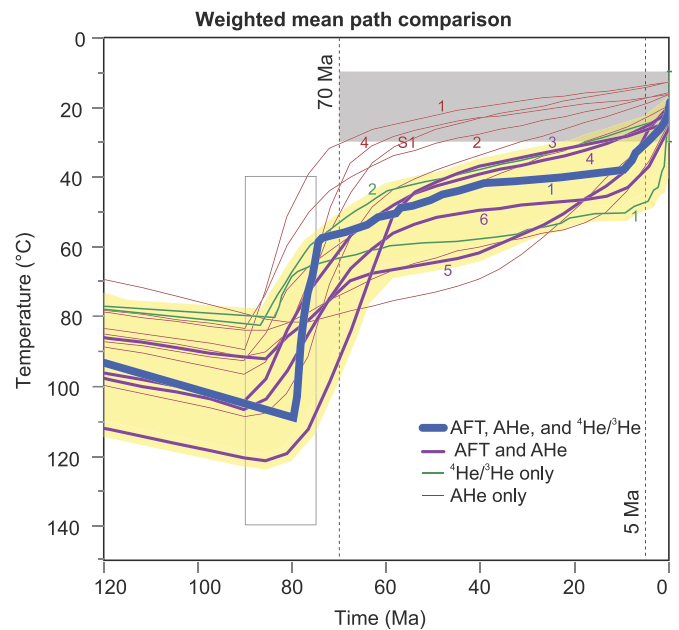


Fig. 7. A weighted mean t - T path comparison for all samples shows inconsistent paths. Models using our new $^4\text{He}/^3\text{He}$ data, the $^4\text{He}/^3\text{He}$ data from Flowers and Farley (2012), all models involving combined AFT and AHe, and about half the AHe-only t - T paths show post-Laramide residence at 40–60 °C from 70 to after 20 Ma, consistent with a “young” Canyon. Four AHe-only best-fit paths are best predicted by t - T paths involving rapid cooling at 70 Ma, consistent with an “old” Canyon (gray band). This range of t - T paths is not physically possible because many of the conflicting t - T paths are from the same location. Our preferred path is the jointly inverted multi-dataset path from sample #1 (blue) suggesting that Separation Canyon rocks reached maximum Laramide burial temperatures of 80–110 °C, resided at post-Laramide temperatures between 40–60 °C from 70 to 6 Ma, and cooled to near-surface temperatures after 5 Ma. (For interpretation of the references to color in this figure legend, the reader is referred to the web version of this article.)

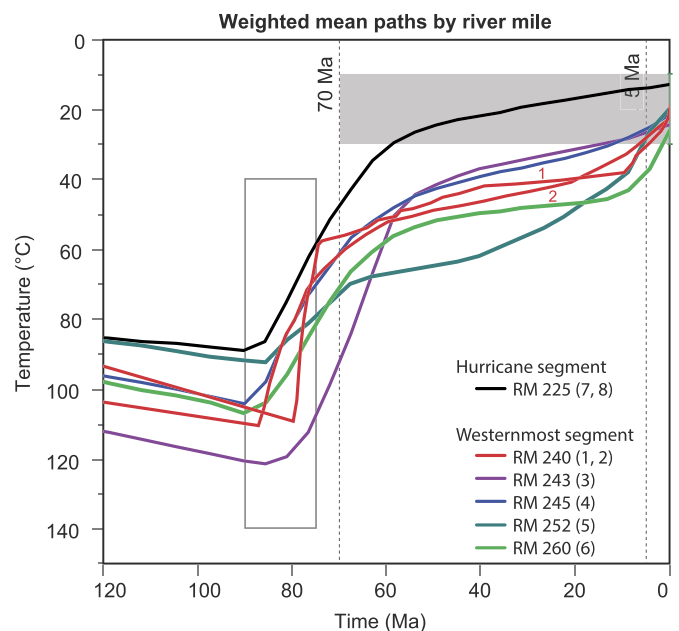


Fig. 8. Synthesis of weighted mean t - T paths by river mile that shows preferred t - T paths based on the combination of multiple analytical techniques. Our preferred path for each sample is shown, including those with adjusted r_{mr0} values (RM 240). Most t - T paths support a “young” Canyon, but post-Laramide residence T varies from 40–70 °C. The black path is from samples #7 and #8 at Diamond Creek and suggests a paleocanyon carved by the Music Mountain paleoriver along the Hurricane segment by ~60 Ma. Our explanation for the varied post-Laramide residence temperatures is ragged northward cliff retreat of the Kaibab escarpment.

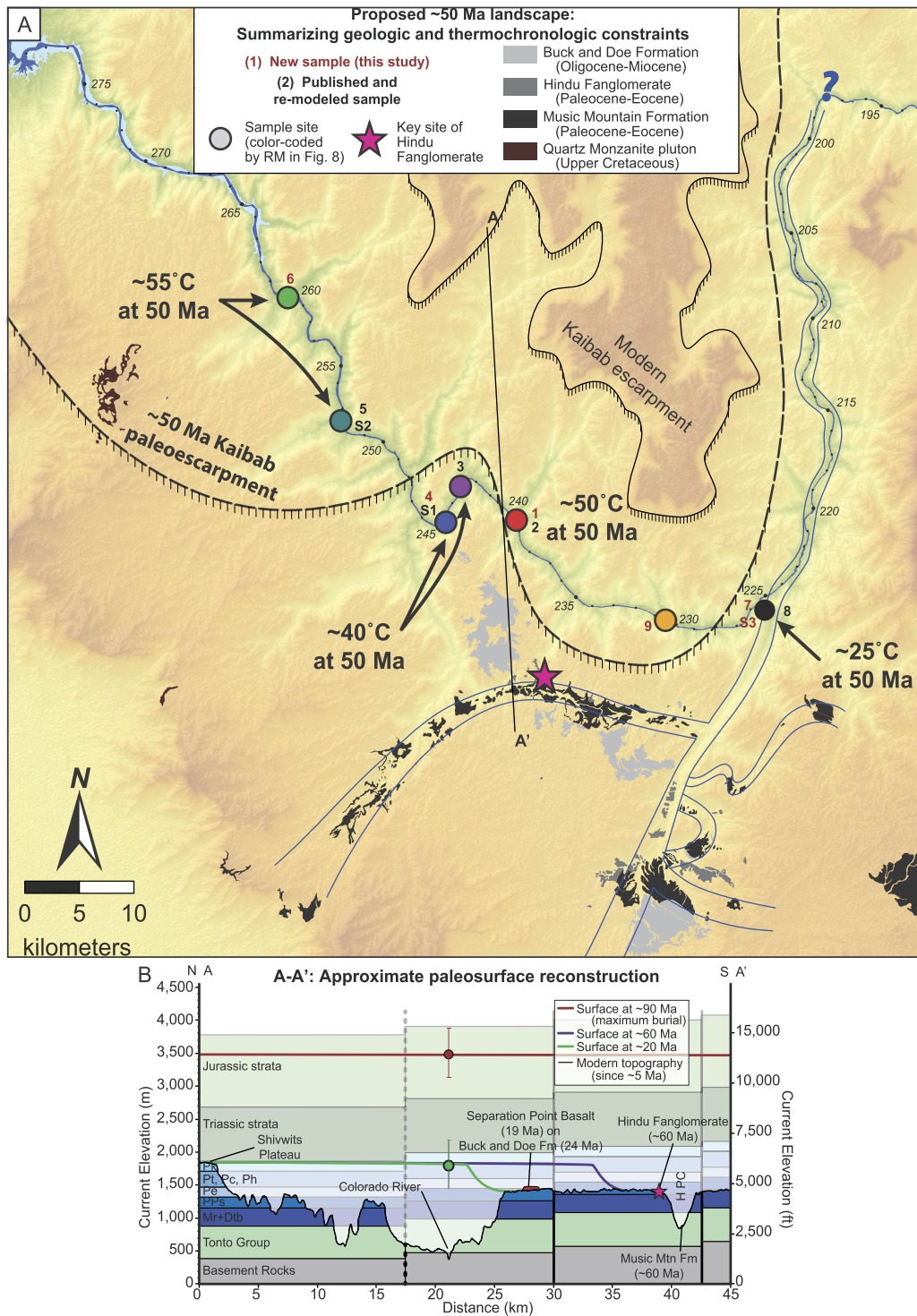


Fig. 9. A) Hypothesis that irregular scarp retreat of the Kaibab escarpment may explain different post-Laramide (~50 Ma) residence temperatures of western Grand Canyon basement samples. Paleocanyons at Diamond Creek and along the Hurricane segment of Grand Canyon explain the cool temperatures of ~25 °C for the combined AFT and AHe data from samples 7 and 8 at ~50 Ma. In contrast, temperatures are ~50 °C at river mile 240 for samples #1 and #2, ~40 °C for samples 3 and 4 at river miles 243–245, and ~60 °C at river miles 252–260, suggesting variable cover by at least ~600 m of upper Paleozoic strata (assuming a 25 °C surface temperature and 25 °C/km geothermal gradient). Red outcrops are a shallowly emplaced Late Cretaceous pluton, indicating appreciable cover at this location. Pink star is key exposure of Hindu Fanglomerate sourced from northern exposures of Pennsylvanian–Permian strata. Paleochannel flow directions and mapping are by Young and Crow (2014). B) N–S cross-section along line A–A', using our preferred t – T path from sample #1 based on combined AFT, AHe, and $^4\text{He}/^3\text{He}$ data and assuming a 25 °C surface temperature and 25 °C/km geothermal gradient to reconstruct possible paleosurfaces above the Colorado River. This cross section includes surficial constraints such as the Separation Point Basalt, Buck and Doe Conglomerate, north-derived Hindu Fanglomerate, and Music Mountain Formation within the 55–65 Ma Hindu paleocanyon. (For interpretation of the references to color in this figure legend, the reader is referred to the web version of this article.)

to completely anneal radiation damage that accumulated during long-term surface residence, this assumed rate of radiation damage annealing is an especially important source of uncertainty in our analysis. This is partly addressed by requiring t – T paths to be

in the Proterozoic so the pre-Laramide thermal history can be accounted for, but cannot be totally reconciled between samples in this region using our current understanding of He diffusion in apatite.

During the modeling process, we noticed that the subset of t - T paths that reached higher temperatures during the Laramide ($>110^{\circ}\text{C}$) tended to reach cooler temperatures ($<30^{\circ}\text{C}$) more quickly than paths that stayed at lower temperatures during the Laramide, demonstrating the difference between starting modeled t - T paths at high temperatures in the Laramide such as those Flowers and Farley (2012) employed versus starting these paths in the Proterozoic to account for the entire thermal history and allowing the data to determine maximum burial temperatures. Fox and Shuster (2014) emphasized that when using the RDAAM, the t - T paths that represent AHe data are sensitive to the range of temperatures reached during maximum burial. These maximum burial temperatures are best constrained by AFT data which provide a valuable co-constraint that directly influence the t - T paths allowed by the AHe and $^4\text{He}/^3\text{He}$ data. The wide range allowed by our Laramide constraint box allows the AFT data to determine maximum burial temperatures and therefore pick the most representative low- T cooling paths following burial for the AHe data using the RDAAM. These t - T paths almost invariably support a “young” Canyon.

Fig. 8 shows weighted mean paths for samples with multiple datasets, color coded by river mile, to help evaluate whether different thermal history model results may reflect real variation in cooling histories. We interpret the “old” Canyon t - T paths at Diamond Creek to be real and to indicate that the Hurricane segment had cooled to 20 – 30°C by 65 – 55 Ma and was carved by the Music Mountain and Hindu paleocanyon system (Karlstrom et al., 2014). Samples at river mile 240 (samples #1 and #2) reside at $\sim 50^{\circ}\text{C}$ after the Laramide. Samples #3, #4, and #51 in the westernmost Grand Canyon have similar low- T post-Laramide residence of $\sim 40^{\circ}\text{C}$ at river mile 243–246. Samples at river miles 250–260 (samples #5 and #6) reside at 60 – 80°C after the Laramide. These temperature differences could plausibly represent real differences in burial depth. A geologic hypothesis capable of explaining different t - T paths in these locations involves ragged cliff retreat of the Kaibab escarpment (Karlstrom et al., 2014). Fig. 9 shows the present-day position and an approximate 50 Ma position of this escarpment that could explain different post-Laramide residence temperatures in westernmost Grand Canyon samples.

6. Conclusions

A diverse set of geologic studies continues to strongly support a 5–6 Ma integration of the Colorado River from the Colorado Plateau to the Gulf of California and carving of the westernmost Grand Canyon in the last 6 million years. The thermochronology of the westernmost Grand Canyon has been controversial, but this paper demonstrates that the thermochronology can be reconciled with compelling geologic field evidence. The application of multiple thermochronology methods, especially new precise $^3\text{He}/^4\text{He}$ data, applied to the same source rocks at Separation Canyon, resolves the debate about the age of westernmost Grand Canyon. The combined data from this location cannot be explained by an “old” Canyon that was carved to within 200 m of its modern depth by 50 Ma; indeed, the new $^3\text{He}/^4\text{He}$ data alone precludes an “old” Canyon (see companion paper Fox et al., 2017). Instead, our best t - T path for this location involves two-stage cooling with both Laramide and <10 Ma pulses. New t - T paths generated by modeling other samples from this study, spanning river mile 230 to 260, also argue strongly for a “young” westernmost Grand Canyon. In contrast, samples at RM 225, within the Hurricane segment of Grand Canyon, are consistent with an “old” 55–65 Ma (Music Mountain age) paleocanyon system that flowed north across the present path of the Grand Canyon as proposed by Karlstrom et al. (2014).

Our best-fitting ‘young’ Canyon thermal history for westernmost Grand Canyon involves: 1) a history of long term, low temperature residence since the Proterozoic (a key difference between our models and previous models; e.g. Flowers and Farley, 2012); 2) peak pre-Laramide burial temperatures of about 80 – 110°C , compatible with burial by about 3 km of Paleozoic and Mesozoic strata; 3) a Laramide cooling episode that took place from 90 – 70 Ma and resulted in cooling to temperatures of 40 – 60°C , compatible with erosional beveling of the Hualapai Plateau to the level of the Esplanade Sandstone by the northward cliff retreat of a ~ 2 km section of upper Paleozoic and Mesozoic rocks; 4) a period of long-term (70 to 10 Ma) residence at temperatures of 40 – 60°C , compatible with burial of samples by about 1 km (600 m to 1.4 km) of lower Paleozoic strata; which is consistent with the persistent fluvial base level observed on the Hualapai Plateau and the absence of a westernmost Grand Canyon; and 5) cooling to near-surface temperatures in the last 5–6 Ma, compatible with the Muddy Creek constraint and the arrival of the Colorado River to the Gulf of California at about 5.3 Ma (Dorsey et al., 2007).

The westernmost Grand Canyon should continue to be an excellent field laboratory for advancing understanding of low-temperature apatite thermochronology and He diffusion in apatite with a complex thermal history. This study highlights a range of continued uncertainties due to relatively low-temperature burial reheating where radiation damage may not be completely annealed, causing complex He diffusion kinetics related to the rate and temperature sensitivity of alpha-recoil damage annealing in apatite. Understanding possible variables that control the retentivity of apatite crystals and variation in $r_{\text{mr}0}$, such as previously unrecognized radiation damage effects, and better understanding of age dispersion are current challenges for modeling apatite thermochronology datasets.

Acknowledgements

Research was funded in part by NSF grants EAR-1348007 and EAR-1347990 (to Karlstrom and Shuster) from the Tectonics Program. We acknowledge laboratory assistance provided by Nick Fylstra. We thank two anonymous reviewers whose comments helped improve the paper.

Appendix A. Supplementary material

Supplementary material related to this article can be found online at <http://dx.doi.org/10.1016/j.epsl.2017.06.051>.

References

- Ault, A.K., Flowers, R.M., 2012. Is apatite U–Th zonation information necessary for accurate interpretation of apatite (U–Th)/He thermochronometry data? *Geochim. Cosmochim. Acta* 79, 60–78. <https://doi.org/10.1016/j.gca.2011.11.037>.
- Babenroth, D.L., Strahler, A.N., 1945. Geomorphology and structure of the East Kaibab monocline, Arizona and Utah. *Bull. Geol. Soc. Am.* 56, 107–150. [http://dx.doi.org/10.1130/0016-7606\(1945\)](http://dx.doi.org/10.1130/0016-7606(1945)).
- Billingsley, G.H., Block, D.L., Dyer, H.C., 2006. *Geologic Map of the Peach Springs 30' x 60' Quadrangle, Mohave and Coconino Counties, Northwestern, Arizona*.
- Blackwelder, E., 1934. Origin of the Colorado River. *Bull. Geol. Soc. Am.* 45, 551–566. <http://dx.doi.org/10.1130/GSAB-45-551>.
- Carlson, W.D., Donelick, R.A., Ketcham, R.A., 1999. Variability of apatite fission-track annealing kinetics, I, experimental results. *Am. Mineral.* 84, 1213–1223. <http://dx.doi.org/10.2138/am-1999-0901>.
- Crossey, L.J., Karlstrom, K.E., Dorsey, R.J., Pearce, J., Wan, E., Beard, L.S., Asmerom, Y., Polyak, V.J., Crow, R.S., Cohen, A., Bright, J., Pecha, M.E., 2015. Importance of groundwater in propagating downward integration of the 6–5 Ma Colorado River system: geochemistry of springs, travertines, and lacustrine carbonates of the Grand Canyon region over the past 12 Ma. *Geosphere* 11, 660–682. <http://dx.doi.org/10.1130/GES01073.1>.
- Darling, A., Whipple, K.X., 2015. Geomorphic constraints on the age of the western Grand Canyon. *Geosphere* 11, 1–19. <http://dx.doi.org/10.1130/GES01131.1>.

- Davis, W.M., 1901. An excursion to the Grand Canyon of the Colorado. *Harvard Museum of Comparative Zoology Bulletin* 38, 106–201.
- Donelick, R.A., O'Sullivan, P.B., Ketcham, R.A., 2005. Apatite fission-track analysis. *Rev. Mineral. Geochem.* 58, 49–94. <https://doi.org/10.2138/rmg.2005.58.3>.
- Dorsey, R.J., Fluette, A., McDougall, K., Housen, B.A., Janecke, S.U., Axen, G.J., Shirvell, C.R., 2007. Chronology of Miocene–Pliocene deposits at split Mountain Gorge, Southern California: a record of regional tectonics and Colorado River evolution. *Geology* 35, 57–60. <http://dx.doi.org/10.1130/G23139A.1>.
- Dutton, C.E., 1882. Tertiary history of the Grand Cañon District. Reprint 1st ed. United States Geological Survey, Santa Barbara, CA and Salt Lake City, UT.
- Elston, D.P., Young, R.A., 1991. Cretaceous–Eocene (Laramide) landscape development and Oligocene–Pliocene drainage reorganization of transition zone and Colorado Plateau, Arizona. *J. Geophys. Res.* 96, 12389. <http://dx.doi.org/10.1029/90JB01978>.
- Farley, K.A., Stockli, D.F., 2002. (U–Th)/He dating of phosphates: apatite, monazite, and xenotime. *Rev. Mineral. Geochem.* 48, 559. LP-577.
- Flowers, R.M., Farley, K.A., 2013. Response to comments on “Apatite $^4\text{He}/^3\text{He}$ and (U–Th)/He evidence for an ancient Grand Canyon”. *Science* 340, 143. <http://dx.doi.org/10.1126/science.1234203>.
- Flowers, R.M., Farley, K.A., 2012. Apatite $^4\text{He}/^3\text{He}$ and (U–Th)/He evidences for an ancient Grand Canyon. *Science* 338, 1616–1619. <http://dx.doi.org/10.1126/science.1229390>.
- Flowers, R.M., Farley, K.A., Ketcham, R.A., 2015. A reporting protocol for thermochronologic modeling illustrated with data from the Grand Canyon. *Earth Planet. Sci. Lett.* 432, 425–435. <http://dx.doi.org/10.1016/j.epsl.2015.09.053>.
- Flowers, R.M., Ketcham, R.A., Shuster, D.L., Farley, K.A., 2009. Apatite (U–Th)/He thermochronometry using a radiation damage accumulation and annealing model. *Geochim. Cosmochim. Acta* 73, 2347–2365. <http://dx.doi.org/10.1016/j.gca.2009.01.015>.
- Flowers, R.M., Wernicke, B.P., Farley, K.A., 2008. Unroofing, incision, and uplift history of the southwestern Colorado Plateau from apatite (U–Th)/He thermochronometry. *Geol. Soc. Am. Bull.* 120, 571–587. <http://dx.doi.org/10.1130/B262311>.
- Fox, M., Shuster, D.L., 2014. The influence of burial heating on the (U–Th)/He system in apatite: Grand Canyon case study. *Earth Planet. Sci. Lett.* 397, 174–183. <http://dx.doi.org/10.1016/j.epsl.2014.04.041>.
- Fox, M., Tripathy-Lang, A., Shuster, D.L., Winn, C., Karlstrom, K., Kelley, S., 2017. Westernmost Grand Canyon incision: testing thermochronometric resolution. *Earth Planet. Sci. Lett.* 474, 248–256. This issue. <http://dx.doi.org/10.1016/j.epsl.2017.06.049>.
- Gautheron, C., Barbarand, J., Ketcham, R.A., Tassan-Got, L., van der Beek, P., Pagel, M., Pinna-Jamme, R., Couffignal, F., Fialin, M., 2013. Chemical influence on α -recoil damage annealing in apatite: implications for (U–Th)/He dating. *Chem. Geol.* 351. <http://dx.doi.org/10.1016/j.chemgeo.2013.05.027>.
- Huntoon, P.W., Billingsley, G.H., Clark, M.D., 1981. Geologic map of the Hurricane fault zone and vicinity, western Grand Canyon, Arizona. *Grand Canyon Assoc.* 1, 48000, 27.
- Huntoon, P.W., Billingsley, G.H., Clark, M.D., 1982. Geologic map of the Lower Granite Gorge and Vicinity. Western Grand Canyon, Arizona.
- Karlstrom, K.E., Crossey, L.J., Embid, E., Crow, R., Heizler, M., Hereford, R., Beard, L.S., Ricketts, J.W., Cather, S., Kelley, S., 2017. Cenozoic incision history of the Little Colorado River: its role in carving Grand Canyon and onset of rapid incision in the past ca. 2 Ma in the Colorado River System. *Geosphere* 13 (1), 49–81. <http://dx.doi.org/10.1130/GES01304.1>.
- Karlstrom, Karl E., Ilg, B.R., Williams, M.L., Hawkins, D.P., Bowering, S.A., Andseaman, S.J., 2003. Paleoproterozoic rocks of the Granite Gorges. In: Beus, S.S., Morales, M. (Eds.), *Grand Canyon Geology*. Oxford University Press, New York, pp. 9–38.
- Karlstrom, K.E., Lee, J.P., Kelley, S.A., Crow, R.S., Crossey, L.J., Young, R.A., Lazear, G., Beard, S.L., Ricketts, J.W., Fox, M., Shuster, D.L., 2014. Formation of the Grand Canyon 5 to 6 million years ago through integration of older palaeocanyons. *Nat. Geosci.* 7, 239–244. <http://dx.doi.org/10.1038/NGEO2065>.
- Kelley, S.A., Chapin, C.E., Karlstrom, K.E., 2001. Laramide cooling histories of Grand Canyon, Arizona, and the Front Range, Colorado, determined from apatite fission-track thermochronology. *Grand Canyon Assoc. Mon.* 12, 37–46.
- Ketcham, R.A., 2005. Forward and inverse modeling of low-temperature thermochronometry data. *Rev. Mineral. Geochem.* 58, 275–314. <http://dx.doi.org/10.2138/rmg.2005.58.11>.
- Ketcham, R.A., Donelick, R.A., Carlson, W.D., 1999. Variability of apatite fission-track annealing kinetics: III. Extrapolation to geological time scales. *Am. Mineral.* 84, 1235–1255.
- Ketcham, R.A., Carter, A., Donelick, R.A., Barbarand, J., Hurford, A.J., 2007. Improved modeling of fission-track annealing in apatite. *Am. Mineral.* 92, 799–810. <http://dx.doi.org/10.2138/am.2007.2281>.
- Lee, J.P., Stockli, D.F., Kelley, S.A., Pederson, J.L., Karlstrom, K.E., Ehlers, T.A., 2013. New thermochronometric constraints on the Tertiary landscape evolution of the central and eastern Grand Canyon, Arizona. *Geosphere* 9, 216–228. <http://dx.doi.org/10.1130/GES00842.1>.
- Longwell, C.R., 1946. How old is the Colorado River? *Am. J. Sci.* 244, 818–835.
- Lucchitta, I., 1966. Cenozoic geology of the upper Lake Mead area adjacent to the Grand Wash Cliffs, Arizona. Ph.D. thesis. State College, Pennsylvania State University, 218 p.
- Lucchitta, I., 1972. Early history of the Colorado River in the Basin and Range Province. *GSA Bull.* 83, 1933–1948.
- Lucchitta, I., Holm, R.F., Lucchitta, B.K., 2013. Implications of the Miocene? Crooked Ridge River of northern Arizona for the evolution of the Colorado River and Grand Canyon. *Geosphere* 9, 1417–1433. <http://dx.doi.org/10.1130/GES00861.1>.
- McDermott, Jacob J., 2011. Microstructural U–Th–Pb geochronology and $^{40}\text{Ar}/^{39}\text{Ar}$ thermochronologic evidence for both Paleoproterozoic and Mesoproterozoic displacement across the Gneiss Canyon shear zone: lower Granite Gorge, Grand Canyon, Arizona. Master's thesis, University of New Mexico. 34 p.
- McKee, E.D., Wilson, R.F., Breed, W.J., Breed, C.S. (Eds.), 1967. *Evolution of the Colorado River in Arizona*. Museum of Northern Arizona Bulletin, vol. 44. 67 p.
- Naeser, C.W., Duddy, I.R., Elston, D.P., Dumitru, T.A., Green, P.F., 1989. Fission-track dating: ages for Cambrian Strata and Laramide and Post-Middle Eocene Cooling events from the Grand Canyon, Arizona. In: *Geology of Grand Canyon, Northern Arizona (with Colorado River Guides): Lee Ferry to Pierce Ferry, Arizona*. American Geophysical Union, pp. 139–144. <http://dx.doi.org/10.1029/FT115p0139>.
- Powell, J.W., 1875. Exploration of the Colorado River of the west and its tributaries. *Smithsonian Institution Annual Report*. 291 p.
- Ritter, W., Märk, T.D., 1986. Radiation damage and its annealing in apatite. *Nucl. Instrum. Methods Phys. Res., Sect. B, Beam Interact. Mater. Atoms* 14, 314–322. [http://dx.doi.org/10.1016/0168-583X\(86\)90601-4](http://dx.doi.org/10.1016/0168-583X(86)90601-4).
- Shuster, D.L., Farley, K.A., 2005. $^4\text{He}/^3\text{He}$ thermochronometry: theory, practice, and potential complications. *Rev. Mineral. Geochem.* 58, 181–203. <http://dx.doi.org/10.2138/rmg.2005.58.7>.
- Shuster, D.L., Flowers, R.M., Farley, K.A., 2006. The influence of natural radiation damage on helium diffusion kinetics in apatite. *Earth Planet. Sci. Lett.* 249, 148–161. <http://dx.doi.org/10.1016/j.epsl.2006.07.028>.
- Spiegel, C., Kohn, B., Belton, D., Berner, Z., Gleadow, A., 2009. Apatite (U–Th–Sm)/He thermochronology of rapidly cooled samples: the effect of He implantation. *Earth Planet. Sci. Lett.* <http://dx.doi.org/10.1016/j.epsl.2009.05.045>.
- Stevens, L., 1983. *The Colorado River in Grand Canyon, A Guide*. Red Lake Books, Flagstaff, AZ.
- Strahler, A.N., 1948. Geomorphology and structure of the West Kaibab fault zone and Kaibab Plateau, Arizona. *Bull. Geol. Soc. Am.* 59, 513–540.
- Vermeesch, P., 2010. HelioPlot, and the treatment of overdispersed (U–Th–Sm)/He data. *Chem. Geol.* 271, 108–111. <http://dx.doi.org/10.1016/j.chemgeo.2010.01.002>.
- Vermeesch, P., Tian, Y., 2014. Thermal history modeling: HeFTy vs. QTQt. *Earth-Sci. Rev.* 139, 279–290. <http://dx.doi.org/10.1016/j.earscirev.2014.09.010>.
- Warneke, N.L., 2015. Timing of erosional episodes in the Marble Canyon and Vermilion Cliffs region from apatite (U–Th)/He thermochronology. Master's thesis, University of New Mexico. 69 p.
- Wenrich, K.J., Billingsley, G., Blackerby, B.A., 1995. Spatial migration and compositional changes of Miocene–Quaternary magmatism in the western Grand Canyon. *J. Geophys. Res.* 100, 10417–10440. <http://dx.doi.org/10.1029/95JB00373>.
- Wernicke, B.P., 2011. The California River and its role in carving Grand Canyon. *GSA Bull.* 123, 1288–1316. <http://dx.doi.org/10.1130/B30274.1>.
- Young, R.A., 1966. *Cenozoic geology along the edge of the Colorado Plateau in northwestern Arizona*. PhD thesis. Washington University. St. Louis, 167 p.
- Young, R.A., 2001. The Laramide–Paleogene history of the western Grand Canyon region: setting the stage. In: Young, R.A., Spamer, E.E. (Eds.), *Colorado River: Origin and Evolution: Grand Canyon*. In: *Grand Canyon Association Monograph*, vol. 12, pp. 7–15.
- Young, R.A., Crow, R.S., 2014. Paleogene Grand Canyon incompatible with Tertiary paleogeography and stratigraphy. *Geosphere*, 664–679. <http://dx.doi.org/10.1130/GES00973.1>.
- Young, R.A., Hartman, J.H., 2014. Paleogene rim gravel of Arizona: age and significance of the Music Mountain Formation. *Geosphere*, 1–22. <http://dx.doi.org/10.1130/GES00971.1>.